Ternary (Water–Acetone–Ethyl Acetate) Liquid–Liquid Equilibrium System in a Micro-Extractor

Abstract

This study aimed to measure the liquid−liquid equilibrium (LLE) data for a ternary (water–acetone–ethyl acetate) system to extract acetone. For this purpose, the experiments were conducted with a feed containing 80 wt.% water and 20 wt.% acetone in a T-shaped micromixer and then in a 0.8 mm microtube. The operational variables, e.g., solvent-to-feed ratio (S/F, 0.33-3.00 v/v) and operating temperature (303.15, 308.15, 313.15 and 318.15 K) were calculated at 0.1 MPa. According to the experimental results, the best selectivity (S) and distribution coefficient (D_2) were achieved at 0.50 v/v and 313.15 K. Besides, the interaction parameters were obtained for the components by fitting UNIQUAC and NRTL models to experimental data. Both models exhibited high levels of accuracy, with standard deviations in the 0.0002-0.0346 range from experimental data. The results obtained from the UNIQUAC and NRTL models were well consistent with experimental data (root mean square deviation were 0.0138 and 0.0116 for UNIQUAC and NRTL models, respectively).

Keywords: Liquid–liquid equilibrium, Microextraction, Thermodynamic modeling, NRTL, UNIQUAC

Accepted Manuscript

1. Introduction

Acetone is a popular organic solvent used in functional cosmetics, painting, pharmaceutical, and plastics industries. Its high polarity enables it to be miscible in water [1]. There are several common acetone production methods, including 2-propanol dehydrogenation through catalytic oxidation. Accordingly, since the end product has a considerable water content, acetone dehydration is still a paramount issue [2].

While obtaining high-purity acetone is challenging due to its high water solubility, numerous processes are applied to produce and purify it. A distillation column is frequently used to separate water and other impurities from acetone, which faces constraints due to high energy costs during distillation despite achieving acceptable acetone purity [3, 4]. Acetone production industries employ a variety of techniques (e.g., membrane technology) for separating acetone from aqueous mixtures [5-7]. Solvent extraction is another beneficial method used to purify and separate components in solutions with low relative volatility, and heat sensitivity, or when distillation is problematic or impossible [8].

Wang et al. [9] reviewed the LLE data for a ternary (water–acetone–diethyl carbonate (DEC)) system at 298.15/303.15/313.15 K and 100 kPa. They also verified experimental LLE data using Bachman and Othmer–Tobias (OT) equations and correlated it with extended and modified UNIQUAC models.

Mafra et al. [10] studied the LLE and tie-line data for a ternary system (water–acetone–cumene [R-methylstyrene or phenol]) at 323.15/333.15 K and 0.1 MPa. The interaction parameters were obtained for the components from experimental data, which were correlated successfully with both UNIQUAC and NRTL models.

Microfluidics has recently emerged as a promising tool to enhance a range of chemical processes (e.g., extraction) in various ways [11-14]. Kakavandi et al. [15] conducted an experimental study on the liquid–liquid two-phase flow patterns and mass transfer of a ternary system (water–propionic acid (PA)–1-octanol) in various novel rectangular T-micromixers. New T-micromixer configurations were made by modifying their junction shapes and creating pits on the mixing channel to reach efficient mixing.

John et al. [16] investigated how mass transfer between two immiscible liquid phases in a microchannel tube was affected by sonication through direct contact with the transducer in the absence of a liquid medium. The highest yield (i.e., 75%) was obtained at 20.3 kHz, 840 mV, and 0.1 ml/min (flow rate).

Sahu et al. [17] compared PA extraction from toluene to water inside a microchannel using a batch system. This design mainly aimed at evaluating the performance of mass transfer in a well-stirred batch vessel as well as in slug/stratified flows inside microchannels. Based on the results, the maximum extraction efficiency (i.e., 72%) was achieved in 4.47 seconds in the stratified flow regime inside a straight Y-junction microchannel.

Herein, ethyl acetate was chosen to explore the LLE data for a ternary system (water–acetone–ethyl acetate) to extract acetone. Consequently, the experiments were performed with 20 wt.% acetone and 80 wt.% water at 303.15/308.15/313.15/318.15 K and S/F 0.33-3.00 v/v. The experiment data was also verified using Hand and OT equations and correlated by UNIQUAC and NRTL models.

2. Materials and methods

2.1. Materials

Acetone and ethyl acetate, both 99%, were bought from Merck. Besides, all experiments used distilled deionized water. The feed contained 20 wt.% acetone and 80 wt.% water, where ethyl acetate was utilized to extract acetone from water. Table 1 lists the specifications of the utilized chemicals in detail.

Table 1. Characteristics of the chemicals.

Chemical name	CAS #	Source	Purity (wt %)	GC analysis (wt %)
Acetone	67-64-1	Merck	≥ 99.5 %	≥ 99.6 %
Ethyl acetate	141-78-6	Merck	≥ 99.8 %	≥ 99.7 %

2.2. Apparatus and procedures

This study was conducted using a micro-extractor in a laboratory water bath to keep the temperature consistent (uncertainty: 0.2 K). The micro-extractor setup consisted of a stainless steel microtube (internal diameter: 0.8 mm; length: 180 cm) and a T-shaped micromixer.

Each experiment involved feeding a well-known mixture composition (i.e., water–acetone–ethyl acetate) into two T-micromixer inputs using a Qis™ DSP100 peristaltic pump passing through the microtube. The residence time was 27 seconds for all experiments according to the feed rate. Feed stream S/F and temperature were set based on the experimental design. Output settlement was allowed upon leaving to ensure equilibrium, separating it into organic and aqueous phases. The samples were diligently collected in both phases for analysis using Agilent 6890N gas chromatography (GC) equipped with 30m×0.25mm DB-WAX/capillary columns and a flame ionization detector (FID). FID involved helium as the carrier and auxiliary gas. Standard uncertainties are as follows: T = 0.2 K, P = 0.9 Pa, and $w_1, w_2, w_3 = 0.0002$.

2.3. Design of Experiments (DOE)

Herein, acetone was separated from water by utilizing ethyl acetate as the solvent at various S/Fs and temperatures (i.e., 303.15, 308.15, 313.15, and 318.15 K). Table 2 lists the operational parameters. These factors were planned and analyzed in Minitab using full factorial design (FFD). Given different levels of the variables (i.e., 2 and 5), there were 20 experiments. The randomized DoE and experimental LLE data are summarized in Table 3.

Table 2. Operating parameters and their values.

Factor	Symbol	Levels
Solvent to feed ratio, v/v	S/F	0.33, 0.50, 1.00, 2.00, 3.00
Temperature, K	T	303.15, 308.15, 313.15, 318.15

Accepted Manuscript

Table 3. Design of experiments using factorial design and LLE data for ternary systems of water (1)+ acetone (2)+ ethyl acetate (3) at pressure $P = 101.2$ kPa.

No.	Manipulated variables		Overall composition			Aqueous phase			Organic phase			Responses	
	S/F, v/v	T, K	w_1	w_2	w_3	$w_1^{aq.}$	$w_2^{aq.}$	$w_3^{aq.}$	w_1^{O}	w_2^{O}	w_3^{O}	D_2	S
1	0.50	303.15	0.5401	0.1350	0.3249	0.6198	0.1362	0.2440	0.2731	0.1310	0.5959	0.96	2.18
2	3.00	318.15	0.2058	0.0514	0.7428	0.7296	0.0899	0.1805	0.0403	0.0393	0.9204	0.44	7.91
3	3.00	313.15	0.2058	0.0514	0.7428	0.6997	0.0601	0.2402	0.0268	0.0483	0.9249	0.80	20.97
4	0.33	313.15	0.6071	0.1518	0.2411	0.6494	0.1321	0.2185	0.3345	0.2787	0.3868	2.11	4.10
5	3.00	303.15	0.2058	0.0514	0.7428	0.6404	0.1198	0.2398	0.0282	0.0235	0.9482	0.20	4.45
6	0.33	303.15	0.6071	0.1518	0.2411	0.6156	0.1451	0.2393	0.5591	0.1897	0.2512	1.31	1.44
7	2.00	308.15	0.2735	0.0684	0.6582	0.6502	0.1002	0.2496	0.0326	0.0480	0.9194	0.48	9.55
8	1.00	303.15	0.4076	0.1019	0.4905	0.6251	0.1278	0.2471	0.1523	0.0715	0.7762	0.56	2.30
9	0.33	318.15	0.6071	0.1518	0.2411	0.6342	0.1489	0.2169	0.2475	0.1901	0.5624	1.28	3.27
10	2.00	303.15	0.2735	0.0684	0.6582	0.6353	0.1222	0.2425	0.0421	0.0340	0.9239	0.28	4.19
11	0.50	313.15	0.5401	0.1350	0.3249	0.6703	0.1114	0.2183	0.1452	0.2066	0.6482	1.85	8.56
12	3.00	308.15	0.2058	0.0514	0.7428	0.6555	0.0951	0.2494	0.0221	0.0336	0.9443	0.35	10.50
13	0.50	318.15	0.5401	0.1350	0.3249	0.6704	0.1313	0.1983	0.1425	0.1463	0.7112	1.11	5.25
14	1.00	308.15	0.4076	0.1019	0.4905	0.6397	0.1111	0.2492	0.1352	0.0911	0.7737	0.82	3.88
15	2.00	313.15	0.2735	0.0684	0.6582	0.6954	0.0713	0.2333	0.0388	0.0667	0.8945	0.94	16.79
16	1.00	313.15	0.4076	0.1019	0.4905	0.6821	0.0852	0.2327	0.0606	0.1230	0.8164	1.44	16.26
17	0.33	308.15	0.6071	0.1518	0.2411	0.6252	0.1403	0.2345	0.5047	0.2169	0.2784	1.55	1.91
18	2.00	318.15	0.2735	0.0684	0.6582	0.7214	0.1004	0.1782	0.0529	0.0526	0.8945	0.52	7.15
19	1.00	318.15	0.4076	0.1019	0.4905	0.6898	0.1105	0.1997	0.1056	0.0927	0.8017	0.84	5.48
20	0.50	308.15	0.5401	0.1350	0.3249	0.6312	0.1254	0.2434	0.2349	0.1672	0.5979	1.33	3.58

Accepted Manuscript

2.4. Thermodynamic models

Experimental data was correlated using NRTL [18] and UNIQUAC [19] models and the LLE was calculated. The intermolecular interaction parameters were regarded as temperature-dependent because the data was measured at two distinct temperatures:

$$\text{NRTL model: } \tau_{ij} = \frac{\Delta g_{ij}}{RT} = A_{ij} + \frac{B_{ij}}{T}; \quad \left(\tau_{ij} \neq \tau_{ji} \text{ and } \tau_{ii} = 0\right) \tag{1}$$

$$\text{UNIQUAC model: } \tau_{ij} = \exp\left(-\frac{a_{ij}}{R}\right) = \exp\left(A_{ij} + \frac{B_{ij}}{T}\right); \quad \left(\tau_{ij} \neq \tau_{ji} \text{ and } \tau_{ii} = 0\right) \tag{2}$$

In the equation above, τ_{ij} and τ_{ji} denote the interaction energy between i and j molecules, A_{ij} and B_{ij} represent binary interaction parameters (BIPs), and T is absolute temperature. Besides, the pure component's surface area/volume, q_i, r_i, and interaction correction factor $q_i{}'$ for the UNIQUAC model were taken from Table 4.

Table 4. Parameters r_i, $q_i$and q_i' for the studied systems.

Component	$\boldsymbol{r_i}$	$\boldsymbol{q_i}$	$\boldsymbol{q_i'}$
water	0.9200	1.400	1.000
acetone	2.5735	2.336	2.336
ethyl acetate	3.4786	3.116	3.116

3. Results and Discussion

3.1. Experimental LLE data

Table 3 presents the LLE data measured for our ternary system (water (1)–acetone (2)–ethyl acetate (3)) in a micro-extractor under various circumstances. All samples underwent analysis at least three times to ensure that experimental measurements were repeatable.

Here, w_i, $w_i^{aq.}$, and w_i^{O} represent i component's overall, aqueous-phase, and organic-phase weight fractions, respectively. Also, i denotes mixture components.

Selectivity (S) and distribution coefficient (D_2) are also given in Table 3 as key parameters for liquid–liquid extraction:

$$D_2 = \frac{w_2^{O}}{w_2^{aq.}} \tag{3}$$

$$S = D_2 \frac{w_1^{aq.}}{w_1^{O}} \tag{4}$$

where w_1 and w_2 represent water and acetone mass fractions, respectively. The experimental LLE data are verified using OT (Eq. (5)) and the Hand (Eq. (6)) correlations:

$$\ln\left(\frac{1 - w_1^{aq.}}{w_1^{aq.}}\right) = a_{OT} \ln\left(\frac{1 - w_3^{O}}{w_3^{O}}\right) + b_{OT} \tag{5}$$

$$\ln\left(\frac{w_2^{aq.}}{w_1^{aq.}}\right) = a_H \ln\left(\frac{w_2^{O}}{w_3^{O}}\right) + b_H \tag{6}$$

where and b_{OT}) and (a_H and b_H) are OT and Hand equation constants, respectively, achieved by data regression [20, 21].

Figs. 1 and 2 compare LLE data and OT/Hand equations. Also, Table 5 provides equation constants and their respective R^2 values. Similar R^2 values indicate LLE data and equations are well consistent.

Accepted Manuscript

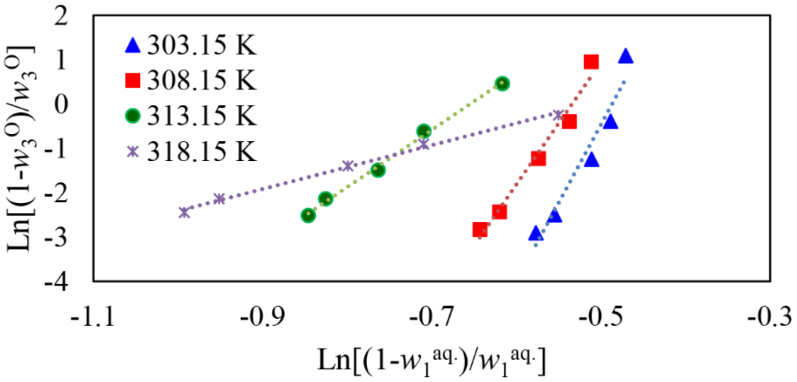

Figure 1. Othmer-Tobias equation for determining the accuracy of equilibrium data; water+ acetone+ ethyl acetate system.

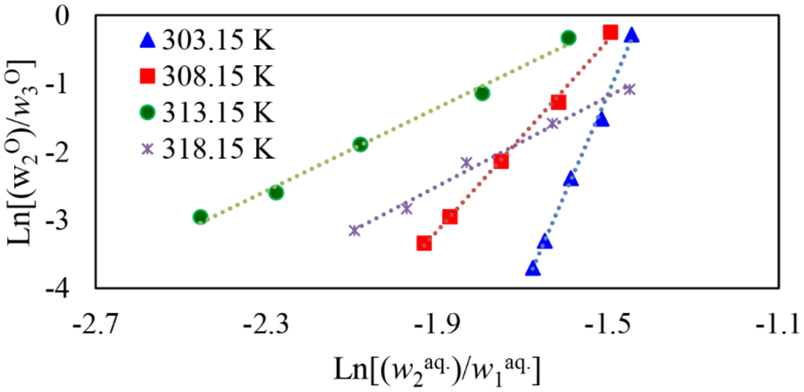

Figure 2. Hand equation for determining the accuracy of equilibrium data; water+ acetone+ ethyl acetate system.

Table 5. The coefficients of Othmer-Tobias and Hand equations and the linear coefficient (R^2) for the investigated systems in this study.

***T*, K**	**Othmer-Tobias**			**Hand**		
	a_{OT}	b_{OT}	R^2	a_H	b_H	R^2
water (1) + acetone (2) + ethyl acetate (3)						
303.15	35.280	17.178	0.9414	14.495	20.587	0.9965
308.15	27.594	14.741	0.9726	6.985	10.110	0.9973
313.15	12.900	8.444	0.9957	3.039	4.417	0.9919
318.15	4.945	2.532	0.9948	3.287	3.740	0.9902

3.2. Statistical analysis and optimization of data

This study explored the effect of S/F and process temperature. The function of the solvent was evaluated using S and D_2, which were statistically analyzed, and their results are provided in Table 6. Also, an analysis of variance (ANOVA) was conducted for them. As seen in Table 6, the responses (i.e., S and D_2) are significantly affected by temperature and S/F.

The impacts of S/F and temperature on S and D_2 are illustrated in Fig. 3. As can be seen, both variables are maximized at 313.15 K. Besides, an increase in S/F led to increased S and decreased D_2. Also, they are optimal (S = 8.56 and D_2 = 1.85) at 313.15 K and S/F of 0.50 v/v, determined by Design-Expert v7.0.0 optimizer.

Accepted Manuscript

Table 6. Analysis of variance (ANOVA) for the distribution coefficient and selectivity of acetone in ethyl acetate solvent.

Source	**DF**	**SS**	**MS**	***F*-Value**	***P*-Value**	**Level of significance**
Distribution coefficient (D_2)						
S/F	4	3.66383	0.91596	98.20	0.000	highly significant
T	3	1.62809	0.54270	58.18	0.000	highly significant
Error	12	0.11193	0.00933			
Total	19	5.40386				
Selectivity (S)						
S/F	4	178.486	44.622	6.06	0.007	highly significant
T	3	297.563	99.188	13.46	0.000	highly significant
Error	12	88.405	7.367			
Total	19	564.455				

script

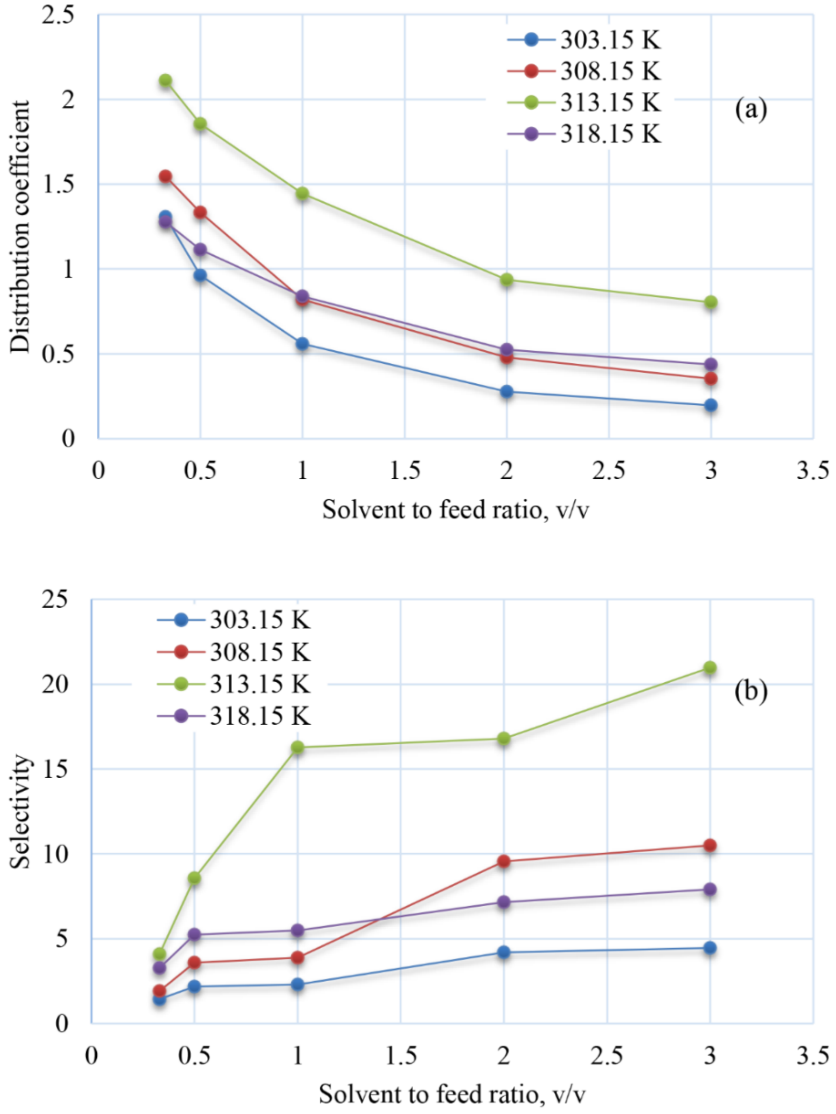

Ac

Figure 3. Effect of ethyl acetate/feed ratio at different temperatures on (a) distribution coefficient, (b) selectivity.

3.3. Thermodynamic modeling of LLE data

BIPs were determined by optimizing the proposed models. Thus, the objective function explains the mean squared difference between measured mass fractions. Also, UNIQUAC and NRTL models were developed for all components in both organic and aqueous phases and were then minimized as:

$$\mathrm{OF} = 100 \times \frac{1}{3D}\sum_{j=1}^{D}\sum_{i=1}^{3}\left(\left(w_{ij}^{\mathrm{aq.,exp}} - w_{ij}^{\mathrm{aq.,calc}}\right)^2 + \left(w_{ij}^{O,\mathrm{exp}} - w_{ij}^{\mathrm{O,calc}}\right)^2\right) \qquad (7)$$

Root mean square deviation (RMSD) was used to compare the models in terms of accuracy:

$$RMSD = \left(\frac{1}{3D}\sum_{j=1}^{D}\sum_{i=1}^{3}\left(w_{ij}^{\mathrm{aq.,exp}} - w_{ij}^{\mathrm{aq.,calc}}\right)^2 + \left(w_{ij}^{O,\mathrm{exp}} - w_{ij}^{\mathrm{O,calc}}\right)^2\right)^{1/2} \qquad (8)$$

where w^{exp} and w^{calc} denote experimental and calculated mass fractions, respectively. Besides, i, j, and D subscripts stand for the components and total number of tie-lines, respectively. Table 7 depicts optimized BIPs for UNIQUAC and NRTL models for current systems. As shown, the same solvent (i.e., ethyl acetate) was used to determine water–acetone interaction parameters. Table 8 lists RMSD values for our ternary system correlated by UNIQUAC and NRTL models (0.0138 and 0.0116, respectively) once intermolecular interaction parameters have been determined.

Table 7. Intermolecular interaction parameters between water+ acetone+ ethyl acetate.

Model	**Component**		**Binary interaction parameter**			
	i	***j***	A_{ij}	B_{ij}, **K**	A_{ji}	B_{ji}, **K**
NRTL	water	acetone	-3.3863	-87.1644	15.2236	-212.0690
	water	ethyl acetate	-3.1306	246.7196	1.4825	-397.7193
	acetone	ethyl acetate	-3.3351	240.1043	1.6129	-508.2520
UNIQUAC	water	acetone	0.4710	-69.2441	0.9573	77.4284
	water	ethyl acetate	1.6979	28.5969	-1.4616	-33.8934
	acetone	ethyl acetate	1.0671	57.5647	-0.7127	-123.2461

Moreover, Fig. 4 illustrates triangular diagrams for our ternary system at 303.15, 308.15, 313.15, and 318.15 K as well as the results of comparison between experimental and NRTL/UNIQUAC-derived data.

Table 8. Liquid-liquid equilibrium data of the systems of water+ acetone+ ethyl acetate and accuracy of models.

T, **K**	**Number of data points**	**RMSD**		D_2	***S***
		NRTL	**UNIQUAC**		
303.15	5	0.0126	0.0132	0.66	2.91
308.15	5	0.0105	0.0143	0.91	5.89
313.15	5	0.0127	0.0175	1.43	13.34
318.15	5	0.0106	0.0090	0.84	5.81

Accepted Manuscript

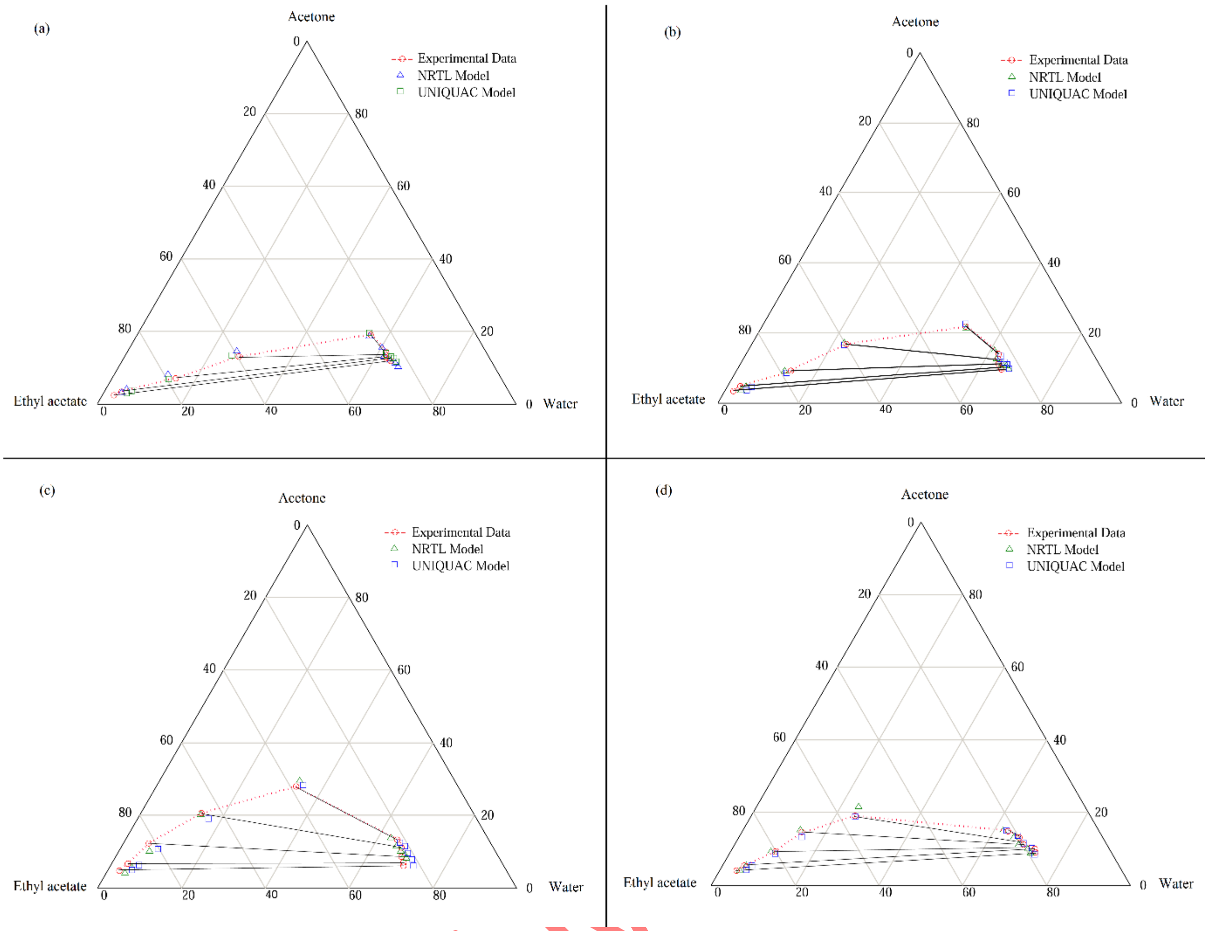

Figure 4. Experimental data of ternary system of water+ acetone+ ethyl acetate and the results of the NRTL and UNIQUAC models at different temperatures; a) 303.15 K, b) 308.15 K, c) 313.15 K, and d) 318.15 K.

Accepted

4. Conclusions

Acetone can be effectively extracted by a micro-extractor in liquid–liquid extraction. The LLE was evaluated by performing experiments at pressure: 0.1 MPa, temperature: 303.15, 308.15, 313.15, and 318.15 K, and S/F: 0.33-3.00 v/v. The optimal extraction conditions were 313.15 K, 0.50 v/v, and acetone: water 20:80, under which D_2 and S were 1.58 and 8.56, respectively. According to the findings, at 313.15 K, constantly increasing water content led to a rapid reduction in S. Finally, it was determined whether UNIQUAC and NRTL models were compatible with LLE data. The results obtained from the above mentioned models were well consistent with experimental data (RMSD = 0.0138 and 0.0116 for UNIQUAC and NRTL models, respectively).

Reference

[1] Weber, M.; Pompetzki, W.; Bonmann, R.; Weber, M.; *Acetone.* Ullmann's Encyclopedia of Industrial Chemistry (Weinheim: Wiley-VCH): **2014,** p. 1–19.

[2] Luyben, W. L., Design and control of the acetone process via dehydrogenation of 2-propanol. *Ind. Eng. Chem. Res.* **2011,** *50* (3), 1206-1218, DOI: 10.1021/ie901923a.

[3] Brunjes, A. S.; Bogart, M. J., Vapor-liquid equilibria for commercially important systems of organic solvents: The binary systems ethanol-n-butanol, acetone-water and isopropanol-water. *Ind. Eng. Chem. Res.* **1943,** *35* (2), 255-260, DOI: 10.1021/ie50398a032.

[4] Xie, S.; Song, W.; Fu, C.; Yi, C.; Qiu, X., Separation of acetone: From a water miscible system to an efficient aqueous two-phase system. *Sep. Purif. Technol.* **2018,** 192, 55-61, DOI: 10.1016/j.seppur.2017.09.056.

[5] Malekpour, A.; Mostajeran, B.; Koohmareh, G. A., (2017). Pervaporation dehydration of binary and ternary mixtures of acetone, isopropanol and water using polyvinyl alcohol/zeolite membranes. *Chem. Eng. Process.: Process Intensif.* **2017,** *118*, 47-53, DOI: 10.1016/j.cep.2017.04.019.

[6] Ray, S.; Ray, S. K., Effect of copolymer type and composition on separation characteristics of pervaporation membranes - a case study with separation of acetone–water mixtures. *J. Membr. Sci.* **2006,** *270* (1-2), 73-87, DOI: 10.1016/j.memsci.2005.06.055.

[7] Koch, K.; Górak, A., Pervaporation of binary and ternary mixtures of acetone, isopropyl alcohol and water using polymeric membranes: Experimental characterisation and modelling. *Chem. Eng. Sci.* **2014,** *115*, 95-114, DOI: 10.1016/j.ces.2014.02.009.

[8] Castro-Puyana, M.; Marina, M. L.; Plaza, M., Water as green extraction solvent: principles and reasons for its use. *Curr. Opin. Green Sustain. Chem.* **2017,** *5*, 31-36, DOI: 10.1016/j.cogsc.2017.03.009.

[9] Wang, C.; Chen, Y.; Cheng, K.; Wen, C., Phase equilibria of the ternary systems of (water+ diethyl carbonate) with acetone, or 2-butanone at four temperatures. *J. Chem. Thermodyn.* **2016,** *102*, 147-154, DOI: 10.1016/j.jct.2016.06.033.

[10] Mafra, M. R.; Krähenbühl, M. A., Liquid− liquid equilibrium of (water+ acetone) with cumene or α-methylstyrene or phenol at temperatures of (323.15 and 333.15) K. *J. Chem. Eng. Data* **2006,** *51*(2), 753-756, DOI: 10.1021/je050500d.

[11] Singh, K. K.; Renjith, A. U.; Shenoy, K. T., Liquid–liquid extraction in microchannels and conventional stage-wise extractors: a comparative study. *Chem. Eng. Process.: Process Intensif.* **2015,** *98*, 95-105, DOI: 10.1016/j.cep.2015.10.013.

[12] Kolar, E.; Catthoor, R. P.; Kriel, F. H.; Sedev, R.; Middlemas, S.; Klier, E.; Priest, C., Microfluidic solvent extraction of rare earth elements from a mixed oxide concentrate leach solution using Cyanex® 572. *Chem. Eng. Sci.* **2016,** *148*, 212-218, DOI: 10.1016/j.ces.2016.04.009.

[13] Ju, M.; Ji, X.; Wang, C.; Shen, R.; Zhang, L., Preparation of solid, hollow, hole-shell and asymmetric silica microspheres by microfluidic-assisted solvent extraction process. *Chem. Eng. J.* **2014,** *250*, 112-118, DOI: 10.1016/j.cej.2014.04.008.

[14] Darekar, M.; Sen, N.; Singh, K. K.; Mukhopadhyay, S.; Shenoy, K. T.; Ghosh, S. K., Liquid–liquid extraction in microchannels with Zinc–D2EHPA system. *Hydrometallurgy* **2014,** *144*, 54-62, DOI: 10.1016/j.hydromet.2014.01.010.

[15] Kakavandi, F. H.; Rahimi, M.; Jafari, O.; Azimi, N., Liquid–liquid two-phase mass transfer in T-type micromixers with different junctions and cylindrical pits. *Chem. Eng. Process.: Process Intensif.* **2016,** *107*, 58-67, DOI: 10.1016/j.cep.2016.06.011.

[16] John, J. J.; Kuhn, S.; Braeken, L.; Van Gerven, T., Effect of fluid properties on ultrasound assisted liquid-liquid extraction in a microchannel. *Ultrason. Sonochem.* **2018,** *42*, 68-75, DOI: 10.1016/j.ultsonch.2017.11.003.

[17] Sahu, A.; Vir, A. B.; Molleti, L. S.; Ramji, S.; Pushpavanam, S., Comparison of liquid-liquid extraction in batch systems and micro-channels. *Chem. Eng. Process.: Process Intensif.* **2016,** *104*, 190-200, DOI: 10.1016/j.cep.2016.03.010.

[18] Renon, H.; Prausnitz, J. M., Local compositions in thermodynamic excess functions for liquid mixtures. *AIChE J.* **1968,** *14* (1), 135-144, DOI: 10.1002/aic.690140124.

[19] Abrams, D. S.; Prausnitz, J. M., Statistical thermodynamics of liquid mixtures: a new expression for the excess Gibbs energy of partly or completely miscible systems. *AIChE J.* **1975,** *21* (1), 116-128, DOI: 10.1002/aic.690210115.

[20] Othmer, D.; Tobias, P., Liquid-liquid extraction data-the line correlation. *Ind. Eng. Chem.*, **1942,** *34* (6), 693-696, DOI: 10.1021/ie50390a600.

[21] Hand, D. B., Dineric distribution. *J. Phys. Chem.* **1930,** *34* (9), 1961-2000, DOI: 10.1021/j150315a009.

Accepted Manuscript